RESEARCH PAPER

LAND COVER AND BURN SEVERITY DYNAMICS OF THE OGAN KOMERING ILIR PEATLANDS FROM 2015 TO 2023 USING SAR AND OPTICAL DATASETS

Mokhamad Y. N. Khakim[1*], Pradanto Poerwono[1], Azhar K. Affandi[1], Muhamad F. Anhar[1], Febri Indrawan[1], Tomi Ardiansyah[1], Takeshi Tsuji[2]

[1] Universitas Sriwijaya, Jl. Palembang-Prabumulih Km. 32, Indralaya, Ogan Ilir, South Sumatra, 30662, Indonesia

[2] University of Tokyo, 113-8654, 7-3-1 Hongo, Bunkyo-ku, Japan

***Corresponding author:** myusup_nkh@mipa.unsri.ac.id

Received: January 20th 2024 / Accepted: July 25th 2024 / Published: October 1st 2024

https://doi.org/10.24057/2071-9388-2024-3217

ABSTRACT. Land cover changes and wildfires have had an increasing impact on the Ogan Komering Ilir Peatland ecosystems in South Sumatra, Indonesia. This study aims to understand the peatland land cover and burn severity dynamics from 2015 to 2023. The random forest method was applied to classify land cover, while the differenced Normalized Burn Ratio (dNBR) was used for mapping fire severity. We combined various satellite data to classify land cover, consisting of Landsat-8, Sentinel-1, and Sentinel-2. Landsat-8 or Sentinel-2 images were also used for the dNBR calculation. We revealed complex climate, human, and restoration interactions in land cover and burn severity fluctuations over 273,799 hectares of the study area from 2015 to 2023. The 2015 El Niño-induced drought led to 21,754 fire hotspots and 2.01% of the area in high-severity burns. In 2016, it reduced tree cover by 10.18% and increased bare/sparse vegetation by 6.11%. The 2019 El Niño event led to 7,893 fire hotspots, lessening unburned areas and worsening burns. Due to the extreme effects of the 2015 drought, restoration efforts between 2016 and 2020 significantly decreased fire hotspots in 2016. Tree cover stabilized, reaching 48.46% by 2020, whereas unburned areas rose to 69.46% in 2018, showing good recovery and lower fire severity. In 2021-2023, fire hotspots were modest relative to El Niño years but increased in 2023. After 2020, tree cover decreased, but other land cover classes fluctuated. Therefore, continual monitoring and adaptive management are critical for reducing negative consequences and increasing ecosystem resilience.

KEYWORDS: peatlands, land cover change, burn severity, remote sensing, restoration

CITATION: Khakim M. Y. N., Poerwono P., Affandi A. K., Anhar M. F., Indrawan F., Ardiansyah T., Tsuji T. (2024). Land Cover And Burn Severity Dynamics Of The Ogan Komering Ilir Peatlands From 2015 To 2023 Using Sar and Optical Datasets. Geography, Environment, Sustainability, 3(17), 6-18

https://doi.org/10.24057/2071-9388-2024-3217

ACKNOWLEDGEMENT: We would like to acknowledge Universitas Sriwijaya for financial support through «Penelitian Hibah Kompetitif», Contract Number: 0096.105/UN9/SB3.LP2M.PT/2023, dated on May 8th 2023. We also thank the European Space Agency (ESA) for providing Sentinel-1 data, anonymous reviewers, and the academic editor for their valuable comments and suggestions.

Conflict of interests: The authors reported no potential conflict of interest.

INTRODUCTION

Peat is an organic material created from incompletely decomposed plant residues that accumulate in wetlands and have a thickness of 50 cm or more (Osaki and Tsuji 2015; Osman 2018). Peat ecosystems play an essential ecological role in sustaining human life, living organisms, and maintaining natural balance. Using peatlands without regard for the environment has harmed the peat ecosystem, resulting in disasters. Due to the 'El Niño phenomenon's prolonged dry seasons, peatland drainage increases fire risk (Khakim et al. 2022; Khakim et al. 2020; Usup et al. 2004). In its natural state, peat is saturated with water. When peat is damaged due to forest removal and drying, water from the peat flows easily, causing the peat area to dry out. As a result, the peat volume will decrease, decreasing the peat surface (Khakim et al. 2020).

Peatland fires are a global concern that must be addressed seriously. Fires caused by 'El Niño 2015 had a significant influence on the hydrological and vegetative conditions (Khakim et al. 2022). The restoration target for the 2016-2020 period is 2.4 million hectares, with Pulang Pisau Regency in Central Kalimantan Province, Musi Banyuasin Regency in South Sumatra Province, Ogan Komering Ilir Regency in South Sumatra Province, and Meranti Islands Regency in Riau Province being prioritized (Dohong 2019). The government accelerated area recovery to mitigate the impact of the 2015 forest and land fires. It restored the hydrological function of peat due to forest and land fires in a systematic, targeted, integrated, and comprehensive manner by establishing BRG by Presidential Regulation Number 1 of 2016 (Peat Restoration Agency 2016).

In the specific case of South Sumatra, the restoration objective encompassed 30 peat hydrological units (PHUs), corresponding to an area of approximately 711,479.55 hectares (Badan Restorasi Gambut 2017). This target represents a significant portion of the overall peat acreage in South Sumatra, estimated to be around 1.2 million hectares. Restoration is achieved by implementing water retention structures, filling open canals, and constructing drilled wells. In rehabilitation, revegetation involves deliberately planting native and adaptable seeds in open peatlands and enhancing plantings in areas of degraded peat forests (Peat Restoration Agency 2016). Nevertheless, El Niño in 2019 resulted in the combustion of the peatland in South Sumatra. In 2019, the Ogan Komering Ilir (OKI) regency in the South Sumatra province had the most significant area burned, which amounted to 194,824 hectares. Musi Banyu Asin and Banyu Asin regencies also had substantial amounts of burning, with 63,091 and 27,705 hectares affected, respectively[1]. Therefore, monitoring restoration efforts to evaluate the impacts on peatlands and detect any resultant alterations is crucial.

Assessment and comprehension of land cover changes and fire intensity in the peatland of South Sumatra are critical for several reasons. First and foremost, this technology facilitates the evaluation of the influence of human activities on these vulnerable ecosystems, hence aiding in the formulation of environmentally conscious land-use strategies (Biancalani and Avagyan 2014; Goldstein et al. 2020; Hapsari et al. 2018; Miettinen and Liew 2010). Additionally, monitoring fire severity is essential in anticipating and preventing peatland wildfire's ecological and public health consequences (Harrison et al. 2020; Picotte et al. 2021; Sirin and Medvedeva 2022). Finally, the observation of these parameters contributes to the conservation of environmental diversity and the preservation of a healthy environment within the region.

Satellite-based remote sensing data, such as radar and optical data, plays an important role in addressing these challenges. ENVISAT ASAR is less developed for C-band SAR data because of its low spatial and temporal coverage in tropical regions. However, on April 3, 2014, the Sentinel-1 C-band satellite was launched, becoming the first to guarantee open data access with a 12-day return acquisition period at the equator and systematic global coverage (Panetti et al. 2014). The JAXA ALOS-2 L-band mission launched on May 24, 2014, to continue the ALOS-1 global forest data-collecting policy (Kankaku et al. 2015). However, JAXA's unacceptably high price strategy may prevent this data from being used as part of a worldwide tropical forest monitoring system.

However, the concurrent accessibility of L- and C-band data presents promising prospects for monitoring and administrating tropical forests. The LiDAR technique is a remote sensing technology that offers the distinct advantage of providing high-resolution Fields (Pu 2021; Zhen et al. 2016). Nevertheless, LiDAR technology incurs significant costs and entails extended processing times (Novero et al. 2019). The European Space Agency's Copernicus program offers a valuable chance to enhance monitoring by providing access to new optical and Synthetic Aperture Radar satellite data that exhibit excellent temporal and spatial resolution (Gomarasca et al. 2019; Shirvani et al. 2019).

The readily available data provides notable benefits in facilitating monitoring endeavors. The European Space Agency's mission includes a diverse array of sensors designed specifically for ground monitoring. The satellites encompass Sentinel-1, equipped with a synthetic aperture radar operating in the C-band frequency, and Sentinel-2, an optical satellite. Landsat 8 can capture images exhibiting diverse levels of spatial resolution. Spatial resolution can vary between 15 and 100 meters, and these variations are accompanied by 11 channels with different spectral resolution levels (Loveland and Irons 2016). The primary benefit of Landsat 8 is its provision of unrestricted access to data.

This study aims to assess the restoration of peatlands in the OKI regency, South Sumatra, Indonesia, by analyzing the alterations in land cover and fire severity from 2018 to 2023. Sentinel-1's radar imaging capabilities guarantee all-weather monitoring, supplemented by high-resolution optical imagery from Sentinel-2 and Landsat-8. This integrated technique allows for a more complete analysis and in-depth evaluation of both land cover changes and burn severity. This synergistic use of satellite data results in a more robust understanding of ecosystem dynamics, allowing for timely and informed decision-making for sustainable land management, fire prediction, and environmental conservation activities.

MATERIALS AND METHODS

Study Area

The OKI Regency experienced the most extensive peat fires in South Sumatra, Indonesia, in 2015 and 2019. The fire hotspots of 2015 and 2019 are presented in Figs. 1a and 1b, respectively. In this study, we selected four peat hydrology units (PHUs), namely PHU S. Burnai – S. Sibumbung, PHU S. Sibumbung – S. Talangrimba, PHU S. Talangrimba – S. Ulakedondong, and PHU S. Ulakedondong – S. Lumpur, within this regency, as seen in Fig. 1. The area encompasses a total area of 273,799 hectares. The peat ecosystem in this region covers a cultivation area of 123,800 hectares and a protected area spanning 149,201 hectares. The peat thickness reaches 500 cm over this region.

Consequently, it has been identified as a priority location for restoration efforts, particularly for the PHU S. Burnai – S. Sibumbung. Nevertheless, a notable alteration in land utilization occurred at this specific site, wherein an area designated for conservation purposes was instead utilized to cultivate oil palm plantations. Hence, mapping land cover becomes of significant importance.

Data

The current study employed a combination of remote sensing data from several sources to classify land cover, incorporating both temporal and spectral variety to achieve precise and reliable results. The image collections consisted of Sentinel-1 (S1), Sentinel-2 (S2), and Landsat-8 (L8) from 2015 through 2023. The Sentinel-1 mission is an operational radar satellite mission managed by the European Space Agency (ESA). Providing synthetic aperture radar (SAR) imagery with diverse polarization modes renders it highly helpful for land cover classification, primarily owing to its capacity to operate well in all weather conditions. The investigated area was provided with Sentinel-1 data from the Copernicus S1 GRD image collection. This framework is based on interferometric wide-swath (IW) GRD images. These images guarantee full information detail with a 10 m pixel spacing, a spatial resolution of 20-22 m, and a temporal resolution of 6-12 days (Wang et al. 2020).

In addition, the Sentinel-2 satellite project, developed by the European Space Agency (ESA), offers high-resolution optical imaging in different spectral bands. Using Sentinel-2

[1]KLHK. (2024). SiPongi (Forest and Forestry Monitoring System), Burnt Area Calculation. https://sipongi.menlhk.go.id/indikasi-luas-kebakaran

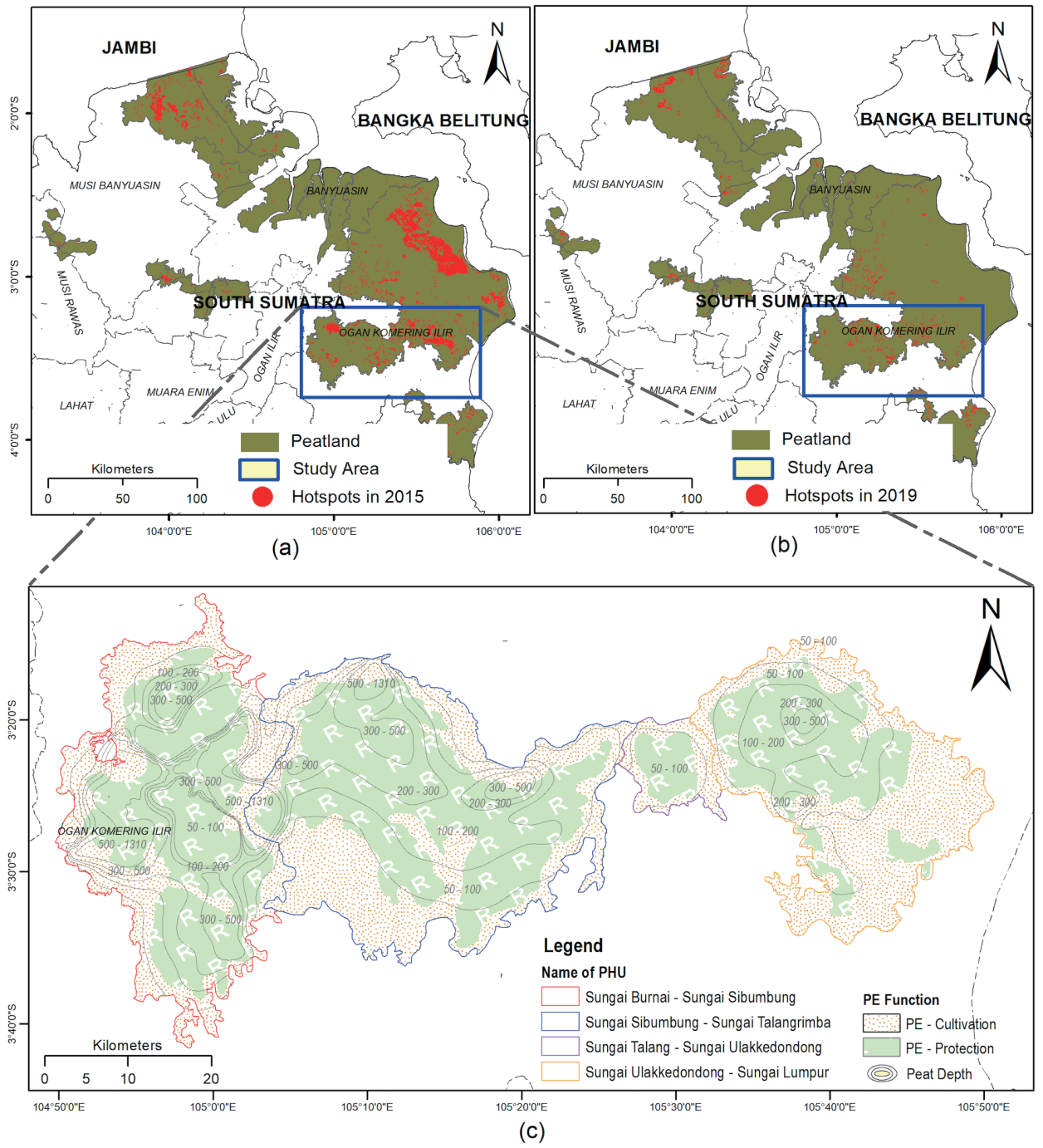

Fig. 1. (a), (b) Fire hotspots over the PHUs of South Sumatra in 2015 and 2019, respectively and (c) peat ecosystem functions of the study area (Peat Restoration Agency 2017) and peat thickness (BBSDLP 2019)

data's multispectral characteristics enables the identification of significant insights related to land cover features. The Sentinel-2 image for our investigation was sourced from the Copernicus S2 level-1 image collection covering the study period. Moreover, the Landsat-8 satellite, jointly operated by the United States Geological Survey (USGS) and NASA, offers optical imagery with a moderate resolution. The use of Landsat-8 data is critical for ongoing land cover monitoring and long-term change detection. The Landsat-8 Surface Reflectance was used from the USGS Landsat 8, Collection 2, Tier 1 dataset image.

Methodology

Preprocessing

The Ground Range Detected (GRD) scenes are a collection of images that have been processed using the Sentinel-1 Toolbox. This processing generates a calibrated and ortho-corrected product made available on the Google Earth Engine (GEE) platform. In our study, we opted for dual polarization modes, specifically VV (vertical-vertical) and VH (vertical-horizontal). In addition, we implemented an improved Lee speckle filter to effectively eliminate speckle noises. This step is crucial in preprocessing synthetic aperture radar (SAR) images. The collection of processed S1 images was converted to a linear power or decibel (dB) scale using the sigma naught (σ^0) parameter. We derived two indices from S1, namely the radar vegetation index (RVI)(Kim et al. 2012) and the normalized ratio procedure between bands (NRPB) (Filgueiras et al. 2019)), which we added to an input image composite.

The Copernicus S2 level-1 image has been orthorectified and radiometrically corrected, which has produced top-of-atmosphere reflectance values (Gatti et al. 2015). It was decided to use Bands 2 to 8, each with an initial spatial resolution of 10 meters. Band QA60 from the S2 1C product was used in an automated cloud masking technique to

ensure data quality (Carrasco et al. 2019). This procedure successfully masked both opaque and cirrus clouds. Clouds and shadows were also masked from Landsat 8 imagery in GEE using the Quality Assessment ("QA_PIXEL") band to mask out pixels with clouds and shadows (Zhen et al. 2023). To create a cloud-free composite image from S1 and S2, we used the median to combine multiple cloud-masked images into one representative image for a year. On the other hand, the mean was used to create an annual S1 image composite.

We calculated the Normalized Difference Vegetation Index (NDVI), Normalized Difference Water Index (NDWI), and Normalized Difference Built-Up Index (NDBI) from the optical S2 and L8 data to increase the accuracy of land cover classification. Besides these auxiliary data, the Inverted Red-Edge Chlorophyll Index (IRECI) and Sentinel-2 Red-Edge Position (S2REP) were calculated from S2 imagery (Frampton et al. 2013). The S1 SAR and S2/L8 optical data, along with their calculated indices, were combined into a yearly composite dataset.

After creating the yearly composite, we applied Principal Component Analysis (PCA) based on the composite. It transformed the original bands into orthogonal or principal components, ranked by their variance. This statistical technique compresses data from many bands into fewer uncorrelated bands. The PCA is also advantageous in improving supervised classification results (Ali et al. 2019). Prior to sampling training points, we added the first three principal component bands to the original composite. We can capture various spectral and structural information about the land cover classes by incorporating 34 bands and indices from multiple sensors and 3 PCA components. The more bands can lead to a more discriminative dataset for classification.

Land Cover Classification

The eight major land cover classifications are tree cover, shrubland, grassland, farmland, built-up, bare/sparse vegetation, water bodies, and herbaceous vegetation. Peat forests, oil palm plantations, rubber plantations, and mangroves were classified as tree cover. We classified shrubs as woody perennial plants with persistent, woody stems and no single, well-defined main stem that grow to a height of less than 5 meters. Grass is any geographical area dominated by natural plants (with no persistent branches or shoots above ground and no definite hard structure). Grasslands include grasslands, prairies, steppes, savannahs, and pastures. Cropland is cultivated land that can be harvested at least once within a year of the first sowing or planting. Buildings, roads, and other manufactured structures, such as railroads, inhabit built-up areas. Furthermore, water class is used to classify different aquatic settings, such as fishponds, rivers, and other bodies of water. Herbaceous wetlands are characterized by natural herbaceous vegetation (coverage of 10% or greater) that is permanently or frequently inundated by fresh or brackish water.

We created 282 feature collections with points representing pixels in those classes. These samples of feature collection have a property called landcover, with values from 1 to 8 representing tree cover, shrubland, grassland, farmland, built-up, bare/sparse vegetation, water bodies, and herbaceous vegetation, respectively. These samples were collected from the RGB composite of the optical imagery and field observation. Furthermore, the classification accuracy was quantitatively estimated by dividing the samples into two random fractions – 70% for training the model and 30% for validation of the predictions.

The Random Forest classification process for peatland analysis in South Sumatra commences with the assembly of a comprehensive input dataset, which encompasses 34 bands, spectral indices, and three PCA-derived components (namely pc1, pc2, and pc3) from Sentinel-1, Sentinel-2, and Landsat-8 imagery. This rich dataset encapsulates a wide range of spectral and radar information for characterizing peatland vegetation and conditions. In the classification stage, a Random Forest method was employed, and notably, all available bands, indices, and PCA components were considered for each tree, totaling 36 features. This method ensures the model leverages all the input data, maximizing its inherent spectral and geographical variety.

After performing the classification, a feature importance analysis was carried out to determine the significance of each feature in distinguishing land over classes. This stage plays a crucial role in identifying the bands, indices, or PCA components that have the most impact on the classification process. By quantifying feature importance scores, we gained valuable insights into the critical elements that contribute to the characterization of peatlands. This, in turn, facilitated the selection and interpretation of features based on data-driven approaches.

The optimal model performance in the Random Forest classification process is dependent on the critical feature of hyperparameter adjustment. To get accurate and robust classification outcomes, it is crucial to precisely tune parameters such as the number of trees, variables per split, bagging fraction, minimum leaf population, maximum number of leaf nodes, and seeds. Exhaustive tuning efforts, often involving grid searches and cross-validation techniques, helped identify the parameter values that maximize classification accuracy while mitigating overfitting risks.

Finally, post-processing techniques are applied to the classification results to refine and enhance their quality. These post-processing steps may encompass spatial smoothing, majority filtering, or object-based analysis tailored to the unique characteristics of peatland regions. The objective is to produce visually coherent and accurate peatland maps suitable for subsequent ecological and environmental assessments or management decisions in South Sumatra's peatland areas.

Mapping Burn Severity

Normalized Burn Ratio (NBR) is used to identify areas of burned vegetation. The NBR for the before and after fires was calculated utilizing optical images, either Landsat-8 or Sentinel-2, using Eq. (1) (Cocke et al. 2005). The NBR value is bounded between -1 and +1, with vegetation contributing the most and burned areas contributing the least. Burn severity can be estimated by calculating the differenced Normalized Burn Ratio (dNBR), as presented in Eq. (2). As shown in Table 1, the values of burn severity indices were categorized into seven distinct severity levels.

$$NBR = (NIR - SWIR) / (NIR + SWIR) \quad (1)$$

$$dNBR = NBR_{prefire} - NBR_{postfire} \quad (2)$$

Table 1. Seven burned severity classes

No	Severity Level	Range
1.	Enhanced Regrowth, High	< -500
2.	Enhanced Regrowth, Low	-250 to -100
3.	Low Severity	-100 to 100
4.	Unburned	100 to 270
5.	Moderate-low Severity	270 to 440
6.	Moderate-high Severity	440 to 660
7.	High Severity	> 660

RESULTS

Optimum parameters and feature importance

We optimized critical hyperparameters in the Random Forest classification context, including decision trees, variables, bagging fraction, leaf population, nodes, and seed value. This step identified the optimum values within defined ranges to assess their influence on classification results. The results were significant, revealing the specific parameter values that, through experimentation and analysis, were found to optimize the Random Forest classification model.

An example of parameter selection for classifying the land cover in 2020 is illustrated in Fig. 2. The study determined that the ideal number of decision trees in the Random Forest ensemble is 270. For the number of variables considered at each split, 15 was identified as the optimal value. The bagging fraction, which controls the proportion of the training data used for building individual trees, performed optimally at 0.9. Regarding the minimum leaf population, the analysis revealed that a minimum of one sample must be present at a leaf node for optimal results. The minimum number of leaf nodes, which indicates the number of terminal nodes in a tree, was observed to be most effective at 100. Lastly, the seed value, which can impact the randomness in the Random Forest, was determined to yield the best results at a value of 301.

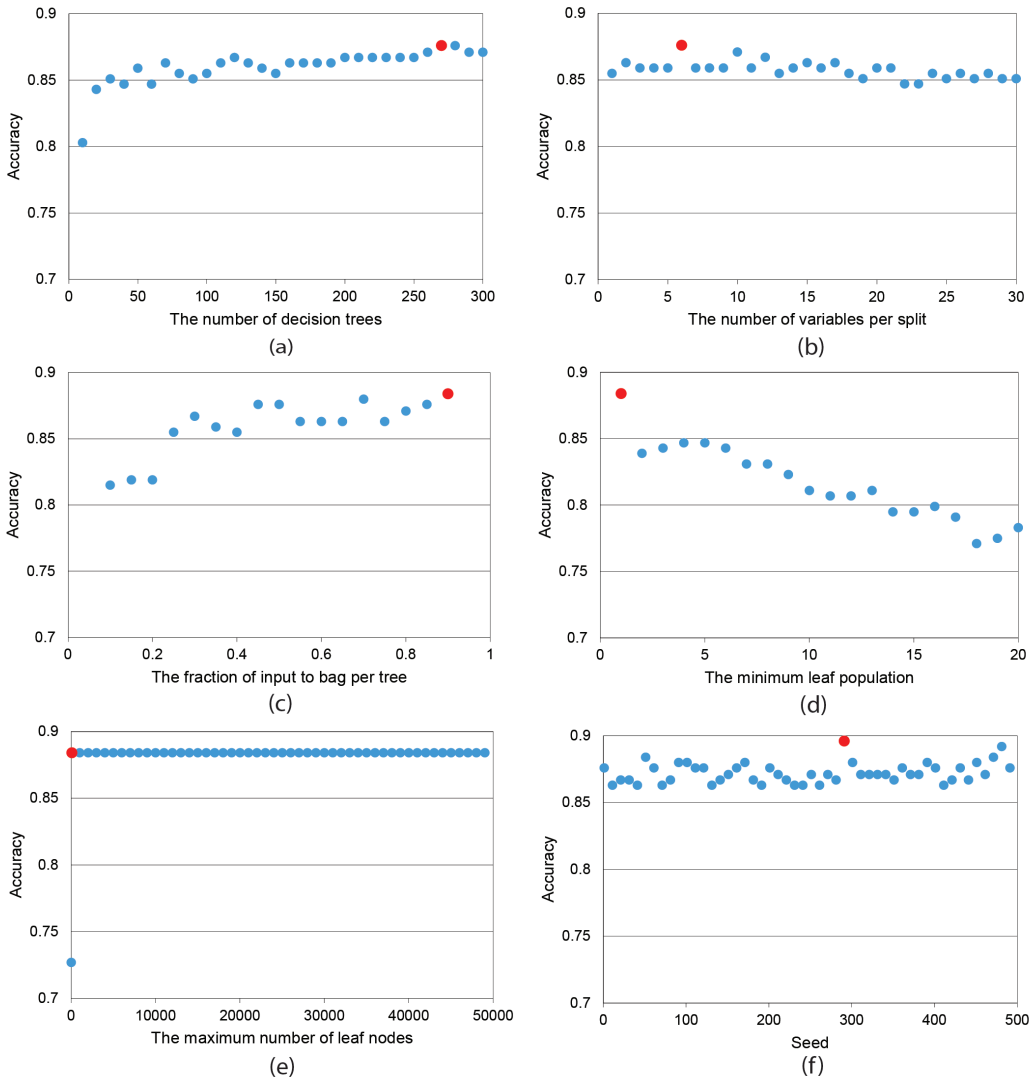

Fig. 2. Selected optimum parameter for the random forest classification

In the context of Random Forest classification analysis, figuring out how discriminative a set of input features from different sources is requires figuring out how relevant each feature is. As shown in Fig. 3, the relative relevance scores reveal unique patterns among these characteristics, offering information on their contributions to land cover classification.

The Sentinel-2 dataset encompasses a collection of spectral bands (B1 to B12) and associated indices (IRECI, S2REP, NDBI of S2, NDVI of S2, NDWI of S2) demonstrating varied significance levels. Bands B5 and B11 significantly have noteworthy relative significance ratings of 3.033 and 3.24, respectively. These bands demonstrate exceptional proficiency in gathering crucial vegetation data, which is fundamental for distinguishing different land cover types. Indices such as the Normalized Difference Vegetation Index (NDVI) derived from Sentinel-2 satellite imagery, which has been assigned a relative relevance value of 2.85, are known to have a substantial impact on assessing the health of vegetation

The Landsat-8 dataset exhibits a collection of significant attributes, notably the surface reflectance bands (SR_B1 to SR_B7) and indices (NDVI of L8, NDWI of L8, NDBI of L8). SR_B3 and SR_B1 are significantly influential, as indicated by their respective relative significance ratings of 3.522 and 3.301. These bands are very important for accurately classifying different types of land cover and describing the land surface's characteristics. An important indication of water-related land cover is the Normalized Difference Water Index (NDWI) produced from Landsat 8 satellite images, with a relative relevance score of 3.047.

Using synthetic aperture radar (SAR) data obtained from Sentinel-1 provides distinctive characteristics with significant relative significance. The VH (Vertical Transmit and Horizontal Receive) method stands out significantly, as indicated by its relative relevance score of 3.205. The (VV – VH) attribute, which denotes the disparity between VV and VH, holds significant significance, as evidenced by its score of 3.115. The SAR features demonstrate exceptional capability in effectively penetrating cloud cover and offering valuable observations regarding surface parameters.

PCA combines Sentinel-1, Sentinel-2, and Landsat-8 data to produce three main components: pc1, pc2, and pc3. Each component contributes to the classification process, with pc1 having a relative importance value of 2.71, pc2 having a score of 2.835, and pc3 having a score of 2.893. These PCA-derived components represent the combination of data from several sources, which jointly improves the classification process.

Land cover accuracy

The high Overall Accuracy (OA) values recorded over several years represent the overall performance of the land cover classification model, as presented in Table 2. These OA values, which range from 76.47% to 91.03%, reflect the model's broad ability to accurately categorize pixels across all land cover categories. It implies that the model adequately represents the landscape's complexity and delivers trustworthy forecasts for diverse land cover types. The Kappa values, which range from 0.71 to 0.89, further emphasize the model's dependability. These results indicate a moderate to significant agreement between observed and anticipated classifications, validating the model's consistency and accuracy in land cover classification.

Across multiple land cover types, the classification model displays remarkable accuracy concerning Producer's Accuracy (PA) and User's Accuracy (UA). The model consistently yields high PA and UA values for tree cover, demonstrating a strong capacity to accurately identify and categorize pixels in this category. This accuracy shows the model's consistency in delivering correct findings and the high likelihood that pixels identified as tree cover represent such vegetation.

The model's accuracy in recognizing shrublands varies with moderate to high PA and UA values, suggesting that environmental conditions or land cover changes may affect its precision. It has reasonable accuracy in categorizing grassland and consistently obtains high PA and UA values, demonstrating its ability to distinguish agriculture from other land cover categories. The model also reliably and accurately identifies built-up regions, demonstrating its dependability in detecting urban or developed areas. However, the accuracy of categorizing bare or sparse vegetation varies, potentially influenced by environmental variables or changes in land cover. The model also reliably classifies water bodies with high PA and UA values, demonstrating its ability to differentiate aquatic characteristics from other land cover categories. For herbaceous wetlands, the model consistently shows high PA and UA values, demonstrating its consistent recognition of these regions over time.

The high OA and Kappa values show that the land cover classification model is accurate and consistent. Over numerous years, the model's consistently high PA and

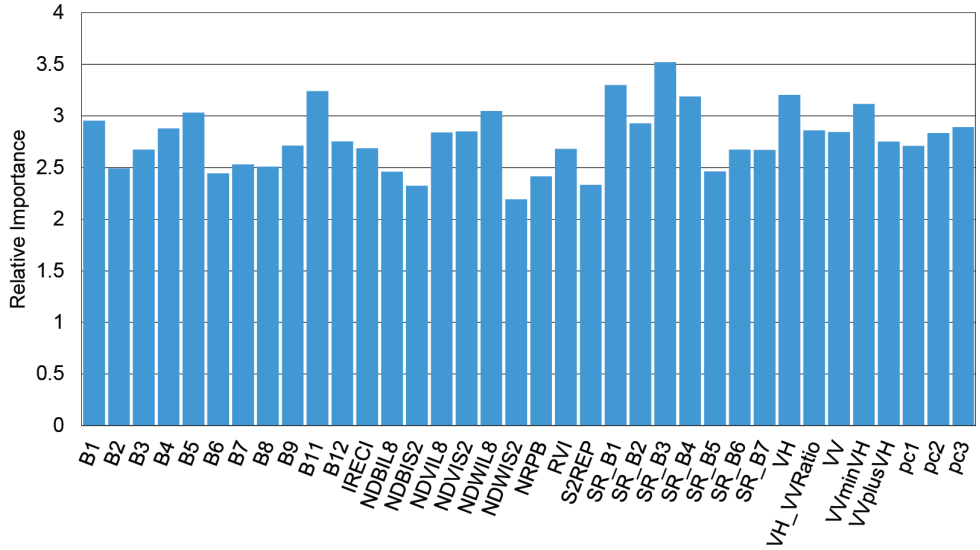

Fig. 3. Relative importance of features as inputs for random forest classification

Table 2. Accuracy measures of land cover classification

Year	Kappa	OA	Tree Cover		Shrubland		Grassland		Cropland		Built-up		Bare / sparse vegetation		Water bodies		Herbaceous Wetland	
			PA	UA	PA	UA	PA	UA	PA	UA	PA	UA	PA	UA	PA	UA	PA	UA
2015	0.74	0.78	0.89	0.71	0.62	0.81	0.54	0.72	0.82	0.93	0.70	0.88	0.40	0.38	1.00	1.00	0.92	0.92
2016	0.71	0.76	0.86	0.80	0.57	0.76	0.67	0.67	1.00	0.75	0.89	0.57	0.50	0.60	1.00	0.95	0.83	0.94
2017	0.76	0.81	0.83	0.78	0.63	0.79	0.53	0.40	1.00	0.92	1.00	0.83	0.48	0.64	1.00	1.00	0.90	1.00
2018	0.81	0.84	0.89	0.84	0.73	0.86	0.69	0.77	1.00	1.00	0.89	0.67	0.65	0.67	1.00	1.00	1.00	0.92
2019	0.81	0.84	0.92	0.79	0.84	0.89	0.82	0.67	0.61	1.00	0.88	0.88	0.58	0.82	1.00	1.00	1.00	1.00
2020	0.89	0.91	0.91	0.94	0.84	0.89	0.96	0.79	0.86	1.00	0.90	0.82	0.77	0.79	1.00	1.00	1.00	1.00
2021	0.87	0.89	0.92	0.87	0.84	0.84	0.96	0.77	0.95	0.95	1.00	0.92	0.60	0.95	0.97	1.00	1.00	0.94
2022	0.81	0.85	0.85	0.73	0.67	0.80	0.72	0.78	0.94	0.88	0.75	0.90	0.76	0.81	1.00	1.00	1.00	0.92
2023	0.84	0.87	0.94	0.89	0.80	0.80	0.89	0.61	0.47	1.00	0.77	0.77	0.72	0.81	1.00	0.98	0.91	1.00

UA values across land cover categories demonstrate its accuracy in identifying and classifying various landscape elements. This result shows that the model captures the dynamics of land cover patterns and provides reliable insights for numerous applications.

Spatiotemporal land cover dynamics

The land cover from 2015 to 2023 is presented in Fig. 4, as determined through the application of Random Forest classification. The spatial and temporal distribution of land cover categories exhibited variation. The tree covers in PHU S. Burnai – S. Sibumbung are primarily comprised of oil palm and rubber plantations, as observed from the field investigation. In contrast, the region of PHU S. Sibumbung - S. Talangrimba was mainly characterized by peatland forest, with a comparatively smaller portion dedicated to plantation activities in the southern part of this PHU.

Peatland regions in four PHUs have exhibited notable changes in land cover. In 2015, an extensive expanse of trees was observed in PHU S. Burnai – S. Sibumbung, amounting to about 16,050 hectares consisting of most oil palm plantations, rubber plantations, and small peat forests. However, throughout the years, a significant reduction in tree coverage has been witnessed, which could be attributed to various factors such as land conversion for plantation purposes and natural events like the El Niño phenomenon, which can contribute to forest fires and deforestation. This decline in tree coverage coincides with an augmentation in shrubland, grassland, and built-up areas, indicating land conversion for plantations, settlements, and other land uses. Additionally, the presence of cloud cover in different years suggests the existence of climatic variations that could potentially impact the detection and analysis of land cover.

In 2019, after the occurrence of the El Niño phenomenon in 2015, a decline in the extent of forested areas was observed in most locations, and this pattern persisted throughout the year 2020. The El Niño phenomenon frequently induces arid conditions, rendering the peatlands more vulnerable to fires, potentially impacting forested areas' extent. However, there was an expansion in grassland, shrubland, and built-up areas, particularly in the regions of KHG Sungai Sibumbung – Sungai Talangrimba and KHG Sungai Ulakkedondong – Sungai Lumpur. These alterations may indicate changes in land utilization, such as the expansion of plantation activities, settlement development, or changes in vegetation types. The conversion of land for agricultural purposes might also contribute to the augmentation of cropland.

The dynamics of land cover appear to be improving in 2021. Several sites had an increase in tree covers, suggesting the possibility of afforestation or natural regeneration, which is encouraging for attempts to conserve peatlands. Other land cover types, such as grassland and shrubland, appear to be expanding, possibly due to continued land use changes and plantation preparation. Furthermore, there was an increase in tree cover in 2023, particularly in KHG Sungai Sibumbung - Sungai Talangrimba, which may result from natural regeneration of forests or plantation growth. It is critical to monitor these trends to ensure that conservation efforts involve the restoration of peat forests and are sustainable.

The relationship between land cover types is dynamic and impacted by various factors, including human activity, conservation initiatives, and climatic phenomena like El Niño. Tree cover can assist in preserving soil moisture and reduce the risk of fire, it is essential for peatland ecosystems, including oil palm and rubber plantations. Peatland conservation faces obstacles posed by expansion into alternative land cover types, specifically settlements and agricultural areas. Restoration programs, climate resilience plans, and sustainable land management techniques are crucial for preserving a healthy balance and safeguarding these essential ecosystems.

The temporal analysis of land cover classes for the overall study area spanning from 2015 to 2023 is presented in Fig. 5. Several noteworthy tendencies can be found in a few of these classes. The tree cover displayed notable temporal fluctuations, with values ranging from a minimum of 40.02% in 2016 to a maximum of 53.12% in 2019. The increase in tree cover in 2019 is indicated as a massive expansion of the oil palm plantation in PHU S. Burnai – S. Sibumbung, which can be seen on the land cover map in Fig. 4. Nevertheless, the decline to 43.56% in 2023 prompts inquiries regarding potential influences such as deforestation or natural disruptions impacting the extent of tree coverage.

In contrast, the shrubland class exhibited steady percentages, ranging from 5.89% to 14.79%, with no significant increasing or decreasing trend. It suggests that there is a stable and persistent land cover within this classification. The data reveals a progressive rise in grassland proportions, commencing at 12.08% in 2015 and

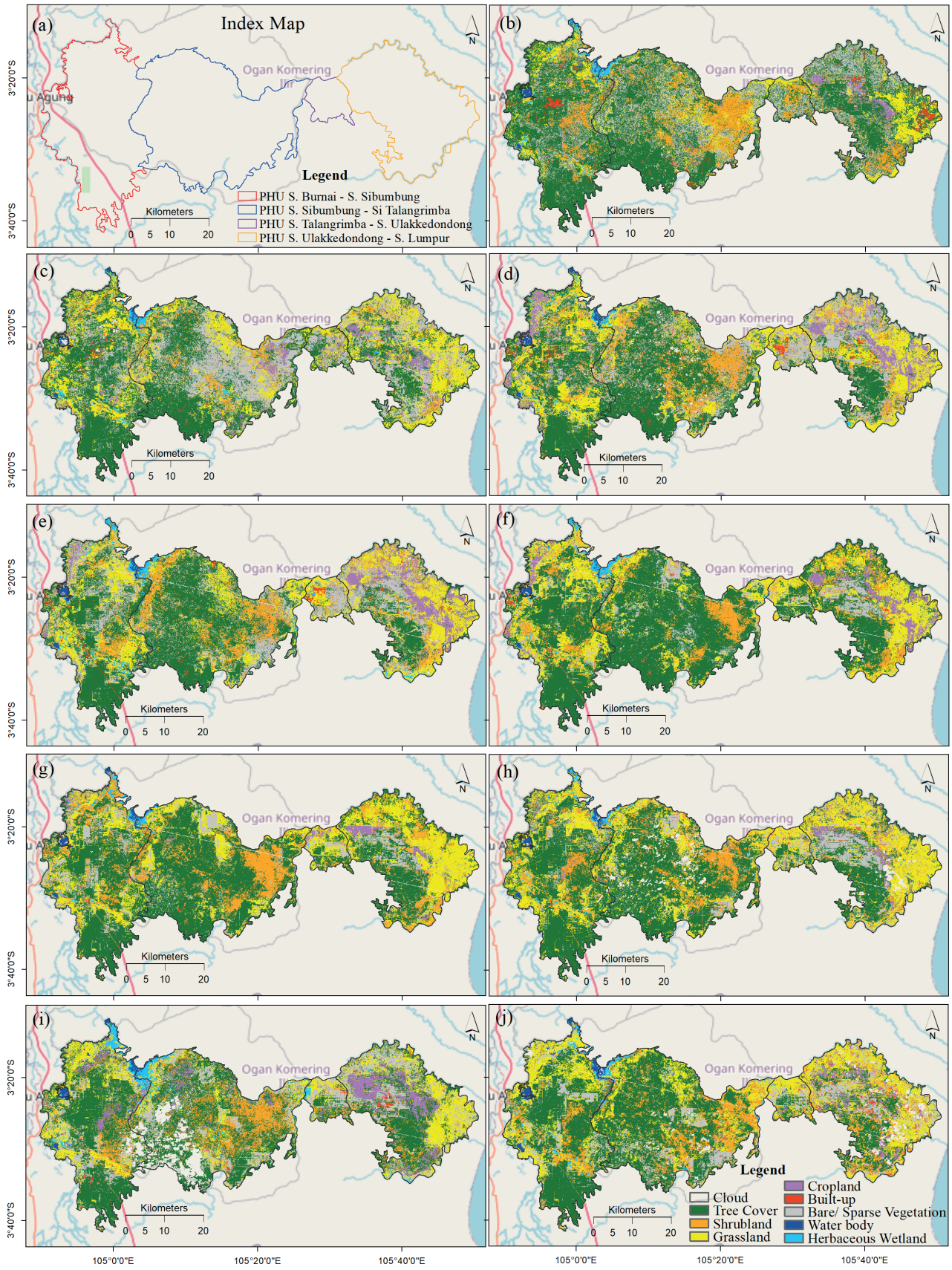

Fig. 4. (a) PHU areas and (b) – (j) classified land cover from random forest method for a period 2015 – 2023, respectively

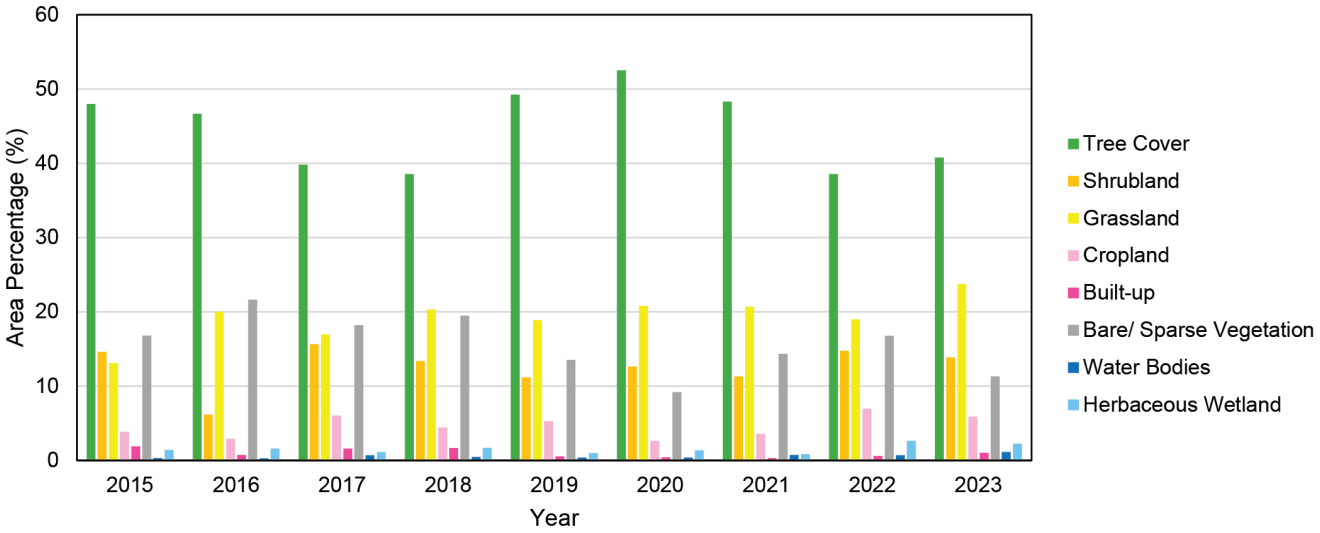

Fig. 5. The variation of land cover percentages for each class from 2015 to 2023

culminating at 24.07% in 2023. This observation implies a potential increase in the extent of grassland ecosystems, possibly driven by alterations in land use patterns, such as changes in forested or shrubland areas into grasslands. Over the observed period, the cropland percentages consistently fluctuated within the 2.04% to 6.23% range. The observed consistency is likely attributable to consistent agricultural techniques or land use policies. The percentage of built-up regions witnessed a marginal rise from 0.36% in 2020 to 0.96% in 2023, indicating a continuing trend of land clearing, especially for plantations. The trend is significant in environmental planning and land use control. The water bodies exhibited notable stability, ranging from 0.34% to 1.13%. This observation suggests that these hydrological features can endure and persist within the broader landscape. The proportions of herbaceous wetlands fluctuated, increasing from 0.36% in 2015 to 1.43% in 2016, followed by subsequent modest fluctuations.

Spatiotemporal Burn Severity Levels

The burnt severity maps for the four-peat hydrological units in the study region from 2015 to 2023 are presented in Fig. 6. PHUs with high fire severity occurred in small areas in S. Burnai-Sibumbung, S. Talangrimba, and S. Ulakkedondong – S. Lumpur, respectively, in 2015, 2019, and 2023. Meanwhile, the PHU with the most significant percentage of areas experiencing high severity is PHU S. Burnai–S. Sibumbung. This severity corresponded to years of El Niño, which caused a severe drought.

Furthermore, a moderate-high severity level had been in a slightly larger area than the high severity level. This severity occurred in the largest region in 2015, especially PHU S. Burnai–S. Sibumbung. Fires of high-moderate severity occurred over all PHUs almost yearly during the study period, even in a tiny percentage of the area. In addition, the trend of the percentages of regions with moderate-low severity was almost the same as that with moderate-high severity, but the percentages were slightly higher. Meanwhile, the low severity of fires had stayed stable over time.

On the contrary, in 2015, 2019, and 2023, as expected, the area did not burn less compared to other years. Unburned areas imply fire resistance and a stable, ecologically stable ecosystem. Meanwhile, low levels of regrowth grew in some PHUs but remained consistant in others. Enhanced regrowth low occurrences were highest in PHU S. Sibumbung–S. Talangrimba and S. Talang–S. Ulakkedondong, but enhanced regrowth high burns were rare and variable. Enhanced regrowth high, identical to enhanced regrowth low, was highest in PHU S. Sibumbung–S. Talangrimba and S. Ulakkedondong–S. Lumpur.

The analysis of burn severity trends from 2015 to 2023 reveals interesting patterns in the temporal distribution of burn severity classifications, as depicted in Fig. 7. Notably, the proportion of high-severity burn regions peaked in 2015 at 2.01% of the landscape. Following that, there was a steady fall, reaching a low of 0.11% in 2017 and 2020. However, there was a modest increase in high-severity burn regions in 2023, recording at 0.95%. Unburned areas, which began at 49.10% in 2015, fluctuated but generally showed an increasing trend in succeeding years, indicating a continuous recovery process.

The data also shows that the trend in moderate-high, moderate-low, and low-severity burn areas is dropping. This decrease indicates a transition from moderate to low burn severity, indicating that these areas are still recovering. Similarly, from 2015 to 2018, the categories of Enhanced Regrowth Low and Enhanced Regrowth High showed constant growth, indicating a period of regrowth and recovery in these areas, followed by minimal changes in succeeding years.

A remarkable contrast arises when comparing 2015 to 2023: whereas high-severity burns peaked at 2.01% in 2015, unburned land accounted for the highest proportion at 69.46% in 2018, indicating significant progress in ecological restoration. This shift reflects a steady tendency toward recovery, as seen by a decrease in the proportions of high and moderate burn severity categories and an increase in unburned and regrowth areas.

DISCUSSION

The relationship between land cover dynamics and fire severity levels exposes interrelated environmental processes and their long-term implications. This study's land cover classification model consistently categorizes different landscape aspects with high OA and Kappa values, demonstrating its dependability in capturing landscape complexity. While the model succeeds at identifying different land cover types such as tree cover, shrubland, grassland, and built-up areas, the model's varying accuracy in recognizing shrublands and sparse vegetation implies susceptibility to environmental shifts or changes in land cover of the study area.

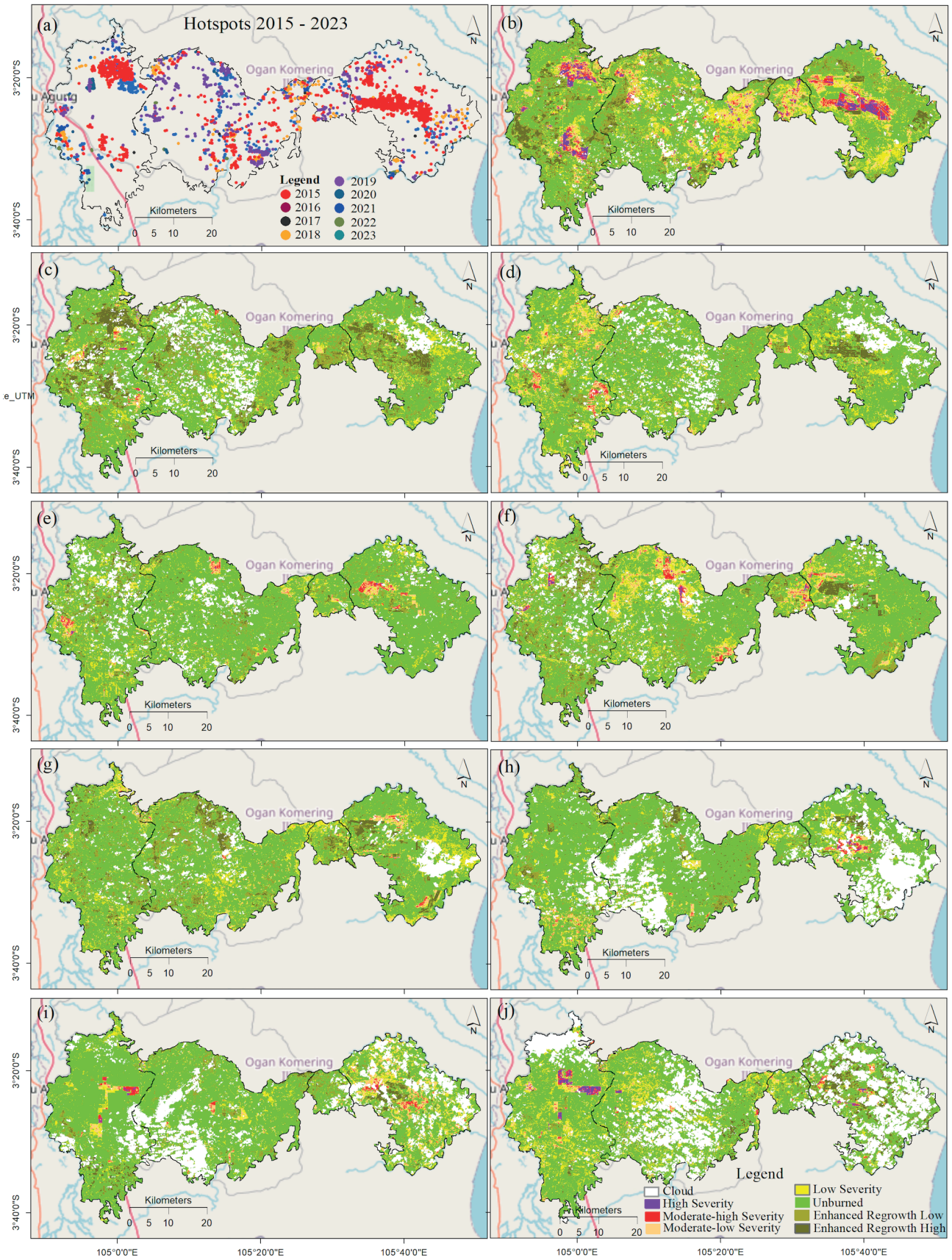

Fig. 6. (a) Fire hotspots and (b) – (j) burned severity in the study area from 2015–2023

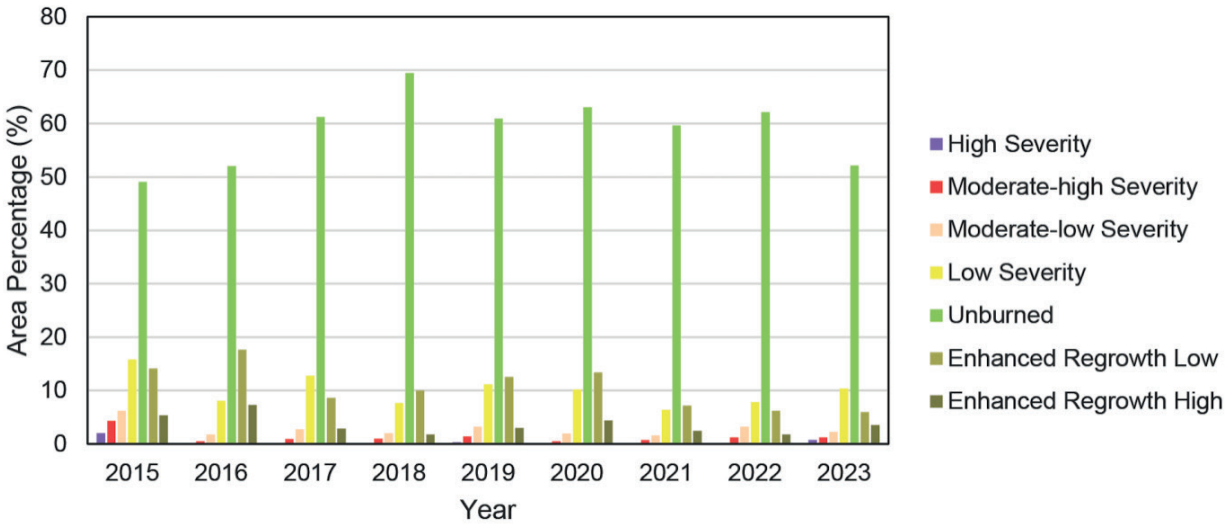

Fig. 7. The variation of area percentages of burn severity from 2015 to 2023

Temporal assessments of land cover transformations reveal subtle changes in tree cover, shrubland, grassland, and built-up areas, particularly in peatland areas. Declines in tree cover and increases in shrubland, grassland, and built-up areas suggest land conversions for plantations or settlements. The peatland conversion to oil-palm plantations also occurred in other sites, such as Riau Province, Indonesia (Numata et al. 2022), Kalimantan, Indonesia, and Peninsular Malaysia (Miettinen et al. 2016). Deforestation and land conversion in peatlands are causing significant loss of natural forest cover, greenhouse gas emissions, and habitat loss for variety of species. In addition, reduced tree cover during El Niño episodes suggests a vulnerability to fires and probable deforestation in peatlands. Peatlands have always had fire as an inherent component of their ecosystems. Agricultural techniques and land clearance are two examples of human activities that have contributed to the dramatic increase in the frequency and severity of flames in the last several centuries (Cole et al. 2019). The ability of peatlands to withstand fire is determined by variables such as the frequency and intensity, as well as the extent of human interference. Undisturbed peatlands demonstrate inherent resilience, but human activities diminish their ability to recuperate after fires. Nonetheless, observed increases in tree cover in some years suggest afforestation or regeneration initiatives are critical for peatland conservation. These variations highlight the dynamic character of landscapes influenced by human activity, conservation efforts, and climatic variations such as El Niño.

The burn severity patterns reported in this study are consistent with the findings of prior research on fire dynamics in tropical peatlands (Page et al. 2009). El Niño events have a substantial impact on fires in Southeast Asian peatlands. These events increase both the frequency and intensity of fires in the region. The fires are more severe during El Niño because of prolonged drought and lower water tables. These conditions make the peat substrates more prone to burning. A significant correlation exists between drought conditions worsened by El Niño occurrences and the increased intensity and spread of fires in tropical peatland regions (Schmidt et al. 2024; Turetsky et al. 2015).

High fire severity during El Niño-induced droughts corresponds to environmental stress, with PHU S. Burnai–S. Sibumbung having the most significant percentage of high-severity burns. Moderate-high severity covers a broader area than high severity, with moderate-low severity having slightly higher proportions. Low-severity fires maintain steady levels over time. Severe fires frequently cause significant changes in the plant communities' composition, promoting the growth of species that are more suited to intense disturbances. On the other hand, fires with minimal intensity typically maintain the plant community's current structure, enabling faster vegetation restoration before the fire (Schmidt et al. 2024). Unburned regions that remain steady over time demonstrate ecological stability and fire tolerance in specific ecosystems. Low-regrowth regions show different tendencies throughout PHUs, with enhanced regrowth levels more prominent in some locales. From 2015 to 2023, the dynamics of burn severity showed a decline in high-severity burn zones, followed by a minor increase in 2023. Moderate-high, moderate-low, and low-intensity burn zones exhibit falling patterns, indicating an ongoing recovery process. The difference between 2015 and 2023, with high-severity burns peaking in 2015 and unburned land reaching its highest share in 2018, demonstrates a persistent trend toward recovery. It provides critical insights into wildfire consequences and ecosystem recovery, aiding in land management decisions and strategic decisions about the recovery and preservation of ecosystems.

This study highlights the importance of understanding the relationship between land cover types and ecosystem dynamics in peatlands. It provides valuable information for local government, BRG, and other stakeholders involved in further restoration programs. Some of the programs must include rewetting drained peatlands, revegetating the landscape, and preparing peatlands without fire. To disable drainage systems, it needs to backfill and obstruct canals. The study underscores the importance of prioritizing restoration efforts in PHU S. Burnai–S. Sibumbung, an area with the highest proportion of burns classified as high severity. Targeted fire prevention and management methods, as well as reforestation and afforestation efforts, are crucial in this area. Planting native tree species that retain soil moisture and reduce fire danger is important. Sustainable land management methods that improve peatland resilience to climate fluctuations, particularly droughts, should be integrated into restoration initiatives. Hydrological restoration measures are also important in mitigating the impacts of climate change on peatlands. Implementing a monitoring system will allow stakeholders to track changes in land cover and fire severity, making timely adjustments to restoration programs. Additionally, engaging the community and educating them on peatland

conservation will generate support for restoration and promote sustainable livelihoods that protect peatland integrity. Peatlands, especially those in the Middle Taiga zone of West Siberia, are important carbon sinks, as (Dyukarev et al. 2019) shown by studying the carbon dynamics of peatland ecosystems. This realization emphasizes the need to preserve intact peatland cover in tropical areas, such as OKI peatland, to lessen the negative impacts of fire occurrences and changes in land cover on carbon sequestration.

CONCLUSIONS

We have successfully performed dynamics of the land cover and burn severity in OKI peatland over the period of 2015 to 2023. The random forest algorithm accurately classified land cover, and the differenced Normalized Burn Ratio (dNBR) robustly delineated burn severity. We summarize our findings from the results as follows:

El Niño-induced drought in 2015 led to high temperatures and increased fire hotspots, causing significant tree cover loss and increased bare/sparse vegetation. In addition, the 2019 El Niño event caused another spike in fire hotspots, reducing unburned areas and increasing burn severity.

Human activities, including oil-palm plantations and agricultural expansion, exacerbated the degradation of natural ecosystems and increased fire risk.

Restoration activities from 2016 to 2020 mitigated the effects of the 2015 drought, resulting in fewer fire hotspots. Post-restoration, tree cover fluctuated, with minor fluctuations and a possible resurgence of fire activity.

The need for sustainable land management practices and stricter regulations is underscored, emphasizing the need for continuous adaptive management to ensure the long-term sustainability of both natural and human-modified landscapes.

REFERENCES

Ali U.A.M.E., Hossain M.A. and Islam M.R. (2019). Analysis of PCA Based Feature Extraction Methods for Classification of Hyperspectral Image. The 2nd International Conference on Innovation in Engineering and Technology (ICIET), Dhaka, Bangladesh. DOI: 10.1109/ICIET48527.2019.9290629

Badan Restorasi Gambut. (2017). Lembar Pengesahan Rencana Restorasi Ekosistem Gambut 7 (Tujuh) Provinsi , Issue September.

BBSDLP. (2019). Map of Peatland of Sumatra Island, Scale 1:50,000.

Biancalani R. and Avagyan A. (2014). Towards Climate-Responsible Peatlands Management. In: Mitigation of Climate Change in Agriculture Series 9. Rome: Food and Agriculture Organization of the United Nations (FAO), http://www.fao.org/3/a-i4029e.pdf

Carrasco L., O'Neil A., Morton R. and Rowland C. (2019). Evaluating Combinations of Temporally Aggregated Sentinel-1, Sentinel-2 and Landsat 8 for Land Cover Mapping with Google Earth Engine. Remote Sensing, 11(3), 288. DOI: 10.3390/rs11030288

Cocke A.E., Fulé P.Z. and Crouse J.E. (2005). Comparison of Burn Severity Assessments Using Differenced Normalized Burn Ratio and Ground Data. International Journal of Wildland Fire, 14(2), 189–198. DOI: 10.1071/WF04010

Cole L.E.S., Bhagwat S.A. and Willis K.J. (2019). Fire in the Swamp Forest: Palaeoecological Insights Into Natural and Human-Induced Burning in Intact Tropical Peatlands. Frontiers in Forests and Global Change, 2(August), 1–15. DOI: 10.3389/ffgc.2019.00048

Dohong A. (2019). Restoring Degraded Peatland in Indonesia: the 3R Approach. Parish, F., Yan, L. S., Zainuddin, M. F. & Giesen, W.(Eds.) RSPO Manual on Best Management Practices (BMPs) for Management and Rehabilitation of Peatlands. 2nd Ed. Kuala Lumpur, RSPO, Kuala Lumpur, 57, 2016–2017.

Dyukarev E.A., Godovnikov E.A., Karpov D.V., Kurakov S.A., Lapshina E.D., Filippov I.V., Filippova N.V. and Zarov E.A. (2019). Net Ecosystem Exchange, Gross Primary Production and Ecosystem Respiration in Ridge-Hollow Complex at Mukhrino Bog. Geography, Environment, Sustainability, 12(2), 227–244. DOI: 10.24057/2071-9388-2018-77

Filgueiras R., Mantovani E.C., Althoff D., Filho E.I.F. and Cunha F.F.d. (2019). Crop NDVI Monitoring Based on Sentinel 1. Remote Sensing, 11(12). DOI: 10.3390/rs11121441

Frampton W.J., Dash J., Watmough G. and Milton E.J. (2013). Evaluating the Capabilities of Sentinel-2 for Quantitative Estimation of Biophysical Variables in Vegetation. ISPRS Journal of Photogrammetry and Remote Sensing, 82, 83–92. DOI: 10.1016/j.isprsjprs.2013.04.007

Gatti A., Naud C., Castellani C., Carriero F., Bertolini A., Nasuti C. and Carriero F. (2015). Sentinel-2 Products Specification Document. Thales Alenia Space, 1–487.

Goldstein J.E., Graham L., Ansori S., Vetrita Y., Thomas A., Applegate G., Vayda A.P., Saharjo B.H. and Cochrane M.A. (2020). Beyond Slash-and-Burn: The Roles of Human Activities, Altered Hydrology and Fuels in Peat Fires in Central Kalimantan, Indonesia. Singapore Journal of Tropical Geography, 41(2), 190–208. DOI: 10.1111/sjtg.12319

Gomarasca M.A., Giardino C., Bresciani M., Carolis G.D., Sandu C., Tornato A., Spizzichino D., Valentini E., Taramelli A. and Tonolo F.G. (2019). Copernicus Sentinel Missions for Water Resources. The 6th International Conference on Space Science and Communication (IconSpac), Italy.

Hapsari K.A., Biagioni S., Jennerjahn T.C., Reimer P., Saad A., Sabiham S. and Behling H. (2018). Resilience of A Peatland in Central Sumatra, Indonesia to Past Anthropogenic Disturbance: Improving Conservation and Restoration Designs Using Palaeoecology. Journal of Ecology, 106(6), 2473–2490. DOI: 10.1111/1365-2745.13000

Harrison M.E., Wijedasa L.S., Cole L.E.S., Cheyne S.M., Choiruzzad S.A.B., Chua L., Dargie G.C., Ewango C.E.N., Honorio C.E.N., Ifo S.A., Imron M.A., Kopansky D., Lestarisa T., O'Reilly P.J., van Offelen J., Refisch J., Roucoux K., Sugardjito J., Thornton S.A. and Page S. (2020). Tropical Peatlands and Their Conservation Are Important in the Context of COVID-19 and Potential Future (Zoonotic) Disease Pandemics. PeerJ, 1–43. DOI: 10.7717/peerj.10283

Kankaku Y., Suzuki S. and Shimada M. (2015). ALOS-2 First Year Operation Result. IEEE International Geoscience and Remote Sensing Symposium (IGARSS), 2, 4121–4124.

Khakim M.Y.N., Bama A.A. and Tsuji T. (2022). Spatiotemporal Variations of Soil Moisture and Groundwater Level in a South Sumatra Peatland, Indonesia During 2015–2018. Geography, Environment, Sustainability, 15(2), 58–70. DOI: 10.24057/2071-9388-2021-137

Khakim M.Y.N., Bama A.A., Yustian I., Poerwono P., Tsuji T. and Matsuoka T. (2020). Peatland Subsidence and Vegetation Cover Degradation as Impacts of the 2015 El Niño Event Revealed by Sentinel-1A SAR Data. International Journal of Applied Earth Observation and Geoinformation, 84(August 2019), 101953. DOI: 10.1016/j.jag.2019.101953

Kim Y., Jackson T., Bindlish R., Lee H. and Hong S. (2012). Radar Vegetation Index For Estimating the Vegetation Water Content of Rice and Soybean. IEEE Geoscience and Remote Sensing Letters, 9(4), 564–568. DOI: 10.1109/LGRS.2011.2174772

Loveland T.R. and Irons J.R. (2016). Landsat 8: The plans, the Reality, and the Legacy. Remote Sensing of Environment, 185, 1–6. DOI: 10.1016/j.rse.2016.07.033

Miettinen J. and Liew S.C. (2010). Status of Peatland Degradation and Development in Sumatra and Kalimantan. Ambio, 39(5), 394–401. DOI: 10.1007/s13280-010-0051-2

Miettinen J., Shi C. and Liew S.C. (2016). Land Cover Distribution in the Peatlands of Peninsular Malaysia, Sumatra and Borneo in 2015 with Changes Since 1990. Global Ecology and Conservation, 6, 67–78. DOI: 10.1016/j.gecco.2016.02.004

Novero A.U., Pasaporte M.S., Aurelio R.M., Madanguit C.J.G., Tinoy M.R.M., Luayon M.S., Oñez J.P.L., Daquiado E.G.B., Diez J.M.A., Ordaneza J.E., Riños L.J., Capin N.C., Pototan B.L., Tan H.G., Polinar M.D.O., Nebres D.I. and Nañola C.L. (2019). The Use of Light Detection And Ranging (LiDAR) Technology and GIS in the Assessment and Mapping of Bioresources in Davao Region, Mindanao Island, Philippines. Remote Sensing Applications: Society and Environment, 13, 1–11. DOI: 10.1016/j.rsase.2018.10.011

Numata I., Elmore A.J., Cochrane M.A., Wang C., Zhao J. and Zhang X. (2022). Deforestation, Plantation-Related Land Cover Dynamics and Oil Palm Age-Structure Change During 1990-2020 in Riau Province, Indonesia. Environmental Research Letters, 17(9). DOI: 10.1088/1748-9326/ac8a61

Osaki M. and Tsuji N. (2016). Peatland Fire Occurrence. Tropical Peatland Ecosystems, Springer Japan. 377-395. DOI: 10.1007/978-4-431-55681-7_25

Osman K.T. (2018). Peat Soil. In: Management of Soil Problems. Springer International Publishing AG, part of Springer Nature. DOI: 10.1007/978-3-319-75527-4_7

Page S., Hoscilo A., Langner A., Tansey K., Siegert F., Limin S. and Rieley J. (2009). Tropical peatland fires in Southeast Asia. Tropical Fire Ecology, 263–287. DOI: 10.1007/978-3-540-77381-8_9

Panetti A., Rostan F., Abbate M.L. and Bruno C. (2014). Copernicus Sentinel-1 Satellite and C-SAR Instrument. IEEE Geoscience and Remote Sensing Symposium, 1, 1461–1464. DOI: 10.1109/IGARSS.2014.6946712

Peat Restoration Agency. (2017). Data Acquisition and Thematic Mapping in KHG Area of Cawang - Lalang River and KHG of Sugihan - Saleh River. Final Report.

Picotte J.J., Cansler C.A., Kolden C.A., Lutz J.A., Key C., Benson N.C. and Robertson K.M. (2021). Determination of Burn Severity Models Ranging from Regional to National Scales for the Conterminous United States. Remote Sensing of Environment, 263(May 2020), 112569. DOI: 10.1016/j.rse.2021.112569

Peat Restoration Agency, Pub. L. No. 1 (2016).

Pu R. (2021). Mapping Tree Species Using Advanced Remote Sensing Technologies: A State-of-the-Art Review and Perspective. Journal of Remote Sensing, 2021. DOI: 10.34133/2021/9812624

Schmidt A., Ellsworth L.M., Boisen G.A., Novita N., Malik A., Gangga A., Albar I., Nurhayati A.D., Ritonga R.P., Asyhari A. and Kauffman J.B. (2024). Fire Frequency, Intensity, and Burn Severity in Kalimantan's Threatened Peatland Areas over Two Decades. Frontiers in Forests and Global Change, 7(February), 1–16. DOI: 10.3389/ffgc.2024.1221797

Shirvani Z., Abdi O. and Buchroithner M. (2019). A Synergetic Analysis of Sentinel-1 and -2 for Mapping Historical Landslides Using Object-Oriented Random Forest in the Hyrcanian Forests. Remote Sensing, 11(19). DOI: 10.3390/rs11192300

Sirin A. and Medvedeva M. (2022). Remote Sensing Mapping of Peat-Fire-Burnt Areas: Identification among Other Wildfires. Remote Sensing, 14(1). DOI: 10.3390/rs14010194

Turetsky M.R., Benscoter B., Page S., Rein G., Van Der Werf G.R. and Watts A. (2015). Global Vulnerability of Peatlands to Fire and Carbon Loss. Nature Geoscience, 8(1), 11–14. DOI: 10.1038/ngeo2325

Usup A., Hashimoto Y., Takahashi H. and Hayasaka H. (2004). Combustion and Thermal Characteristics of Peat Fire in Tropical Peatland in Central Kalimantan, Indonesia. Tropics, 14(1), 1–19. DOI: 10.3759/tropics.14.1

Wang J., Xiao X., Liu L., Wu X., Qin Y., Steiner J.L. and Dong J. (2020). Mapping Sugarcane Plantation Dynamics in Guangxi, China, by Time Series Sentinel-1, Sentinel-2 and Landsat images. Remote Sensing of Environment, 247(June), 111951. DOI: 10.1016/j.rse.2020.111951

Zhen Z., Quackenbush L.J. and Zhang L. (2016). Trends in Automatic Individual Tree Crown Detection and Delineation-Evolution of LiDAR Data. Remote Sensing, 8(4), 1–26. DOI: 10.3390/rs8040333

Zhen Z., Chen S., Yin T. and Gastellu-etchegorry J. (2023). Globally Quantitative Analysis of the Impact of Atmosphere and Spectral Response Function on 2-Band Enhanced Vegetation Index (EVI2) over Sentinel-2 and Landsat-8. ISPRS Journal of Photogrammetry and Remote Sensing. 205(November 2023), 206–226. DOI: 10.1016/j.isprsjprs.2023.09.024